King's Research Portal

Link to publication record in King's Research Portal

Energy Efficient UAV Communication with Energy Harvesting

Zhaohui Yang, Wei Xu, and Mohammad Shikh-Bahaei

Abstract—This paper investigates an unmanned aerial vehicle (UAV)-enabled wireless communication system with energy harvesting, where the UAV transfers energy to the users in half duplex or full duplex, and the users harvest energy for data transmission to the UAV. We minimize the total energy consumption of the UAV while accomplishing the minimal data transmission requests of the users. The original optimization problem is decomposed into two subproblems: path planning subproblem and energy minimization subproblem with fixed path planning. For path planning subproblem, the optimal visiting order is obtained by using the dual method and the trajectory is optimized via the successive convex approximation technique. For energy minimization subproblem with fixed path planning, we firstly obtain the optimal portion of data transmission time within the entire procedure and the optimal transmission power of each user. Then, the the energy minimization subproblem is greatly simplified and it is efficiently solved via a one-dimensional search method. Simulation results are illustrated to verify the theoretical findings.

Index Terms—UAV communication, energy efficiency, energy harvesting, full duplex, straight flight.

I. INTRODUCTION

With the explosive growth of data traffic, unmanned aerial vehicle (UAV) communication has been deemed as a promising technology for future wireless communication networks [1]–[3]. Both spectral and energy efficiency can be improved in scenarios where mobility of UAVs and line-of-sight (LoS)-dominating ground channel characteristics are well explored [4]–[8]. More specifically, UAVs can be utilized in various applications, such as data collection [9]–[12], wireless power transfer [13]–[20], relaying [21]–[24], device-to-device communications [25], caching [26], [27], and mobile edge computing [28].

One line of work in the existing literature about UAV communication is UAV-aided ubiquitous coverage [29]–[34], where the UAVs are deployed to assist existing terrestrial communication infrastructure. To fully exploit the degrees of freedom for designing UAV-enabled communications, it

Z. Yang and M. Shikh-Bahaei are with Centre for Telecommunications Research, King's College London, London WC2R 2LS, U.K. (Emails: {yang.zhaohui, m.sbahaei}@kcl.ac.uk).

W. Xu is with the National Mobile Communications Research Laboratory, Southeast University, Nanjing 210096, China (Email: wxu@seu.edu.cn).

is crucial to investigate resource allocation in UAV-enabled wireless communication networks. In [29], the altitude of UAV was optimized to provide maximum coverage on the ground. To maximize the coverage using the minimum transmit power, an optimal location and altitude placement algorithm was investigated in [30] for UAV-base stations (BSs). With different quality-of-service (QoS) requirements of users, authors in [31] studied the three-dimension (3D) UAV-BS placement that maximizes the number of users in the coverage. Exploiting the flexibility of UAV placement, the number of UAVs required for serving a certain area was considered in [32]. To further consider network delay, the optimal placement and distribution of cooperative UAVs was presented in [35]. In delay-constrained communication scenarios, [36] investigated the fundamental throughput-delay tradeoff in UAV-enabled communications. The authors in [37] solved the mission completion time optimization for multi-UAV-enabled data collection. The UAV trajectory was optimized in [38] for parameter estimation in wireless sensor networks.

On the other hand, energy saving is critical for UAV communications especially in Internet of Things applications [9]. In order to prolong the lifetime of a sensor network, wireless energy consumption was minimized in [10]. Under a more practical energy consumption model of the UAV, it was pointed out that the propulsion energy is much larger than the communication-related energy [39]. Therefore, to minimize the dominating component of energy consumption, the authors in [11] minimized the total flight time of a UAV while allowing sensors to successfully upload a certain amount of data. Further considering the energy consumption of both user and UAV, the tradeoff between the propulsion energy and the wireless energy of the served user was investigated in [12]. There are two major differences between this paper and [12]. One difference is that this paper investigates the total energy minimization for the rotary-wing UAV, while the fixed-wing UAV was adopted in [12]. The other difference is that this paper considers the general multiuser case, while only single user was investigated in [12].

Recently, energy harvesting [40]–[45] has received a great deal of attention in prolonging the lifetime of low-power devices. Different from conventional wireless powered communication network (WPCN), UAV-enabled WPCN can exploit the mobility of UAVs to further improve the system performance [13]–[17]. In [13] and [14], the minimal uplink throughput among all users was maximized for UAV-enabled WPCN. Considering weighted harvest-then-transmit protocol, the sum throughput of all users was maximized in [15]. To further consider the tradeoff between mission completion time and

energy consumption, the energy-time region was obtained via jointly optimizing the UAV trajectory, user scheduling and time allocation [16]. For multi-UAV-enabled WPCN, the minimal throught maximization problem was investigated in [17]. The total amount of harvested energy for all devices was maximized during a finite charging period for UAV communication in [18], and alternatively the minimal harvested energy among all devices was optimized [19]. However, the contributions in [13]–[19] ignored the UAV height optimization.

In this paper, we study a rotary-wing UAV communication system with energy harvesting, where the propulsion energy is explored and UAV height is optimized. The UAV serves as a data collector for multiple users. It broadcasts wireless energy to each user, while the user utilizes the harvested energy to transmit data to the UAV. The contributions of this paper are summarized as:

1) We formulate the problem of energy minimization that jointly optimizes the UAV trajectory, user transmission power, and mission completion time. For the communication between the UAV and each user, half-duplex (HD) and full-duplex (FD) modes are investigated.

2) The analytical models for the propulsion energy consumption of a rotary-wing UAV with acceleration and deceleration are derived for straight flight and vertical flight. To obtain the optimal visiting order of gathering data from all users, the dual method is adopted.

3) For HD, the optimal relationship between the energy harvesting time and the transmission time is revealed. For FD, the optimal transmission time is obtained. These findings ensure that the optimal solution of UAV height to the energy minimization problem can be effectively obtained via a one-dimensional (1D) search.

The rest of this paper is organized as follows. In Section II, we introduce the system model and problem formulation. Path planning and energy minimization with fixed path planning are addressed in Section III and Section IV, respectively. Numerical results are shown in Section V and conclusions are finally drawn in Section VI.

II. SYSTEM MODEL AND PROBLEM FORMULATION

We consider a rotary-wing UAV-enabled wireless communication system with one UAV serving a set $\mathcal{K}$ of K users. The UAV serves as a data collector gathering information data from all users. In the downlink the UAV transfers wireless energy to charge the users, while in the uplink the users utilize the harvested energy to transmit wireless information to the UAV. Without loss of generality, we consider a 3D Cartesian coordinate system such that the location of user k is fixed at $(x_k, y_k, 0)$ and the initial location of the UAV, point A_0, is at (x_0, y_0, H), as shown in Fig. 1. The UAV returns back to point A_0 after the entire procedure of energy transfer and uplink data reception for all K users.

To gather data from all users, the UAV visits all K locations in $K+1$ stage. In the first K stages, the UAV sequentially collect data from K users. The data collecting order is denoted by $\pi_1, \cdots, \pi_K$. In the last $(K+1)$-th stage, the UAV flies back to the initial point and then it can start over again from the first user.
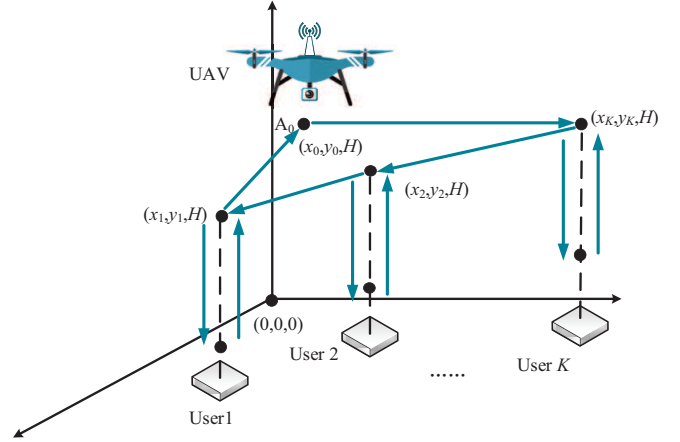
Fig. 1. A UAV-enabled wireless communication system.
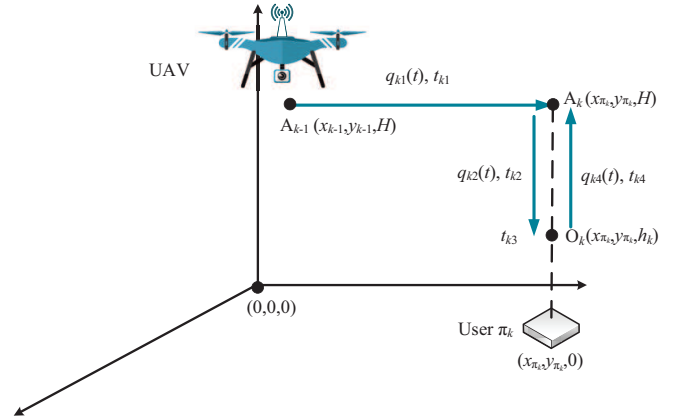
Fig. 2. Fly-hover-communicate protocol.

A. Fly-Hover-Communicate Protocol

The fly-hover-communicate protocol is adopted, i.e., the UAV first flies to a position close to the user and then the UAV broadcasts energy while the user transmits data. In particular, the fly-hover-communicate protocol contains four steps when the UAV collects data from each user.

For the k-th $(k \leq K)$ stage, the UAV needs to collect data from user π_k. In the first step, the UAV straight flies[1] from the location A_{k-1} $(x_{\pi_{k-1}}, y_{\pi_{k-1}}, H)$ to a point A_k $(x_{\pi_k}, y_{\pi_k}, H)$ with trajectory $q_{k1}(t)$ and time duration t_{k1}, as shown in Fig. 2. In the second step, to increase the energy harvesting efficiency, the UAV decreases its height to point O_k $(x_{\pi_k}, y_{\pi_k}, h_k)$ with trajectory $q_{k2}(t)$ and time duration t_{k2}. In the third step, the UAV staying stably at point O_k communicates with the user with time duration t_{k3}. In the

---

[1]The straight flight is considered because straight line is the shortest between two points. Thus, the straight flight is always energy saving for propulsion energy consumption.

fourth step, the UAV increases its hight from point O_k to point A_k at height H with trajectory $q_{k4}(t)$ and time duration t_{k4}. Point A_k is viewed as the initial point to gather data from user π_{k+1}. Note that the UAV increases its height to H because it is the allowed flying height to avoid collision with other UAVs or high buildings. Since the trajectories $q_{k1}(t)$, $q_{k2}(t)$, and $q_{k4}(t)$ are one dimension, we can set the initial location as $q_{k1}(0) = q_{k2}(0) = q_{k4}(0) = 0$ by choosing different reference points.

According to Appendix A, propulsion energy for straight flight in the first step can be expressed as $E_1(q_{k1}(t), t_{k1})$ defined in (A.8). For boundary constraints in $q_{k1}(t)$, we have

$$q_{k1}(t_{k1}) = d_{\pi_{k-1}\pi_k}, v_{k1}(0) = v_{k1}(t_{k1}) = 0, \qquad (1)$$

where $d_{\pi_{k-1}\pi_k} = \sqrt{(x_{\pi_k} - x_{\pi_{k-1}})^2 + (y_{\pi_k} - y_{\pi_{k-1}})^2}$ is the distance between A_{k-1} and A_k, $v_{k1}(t)$ is the velocity at time t and we denote $\pi_0 = 0$. In the second step, the vertical descent energy is $E_2(q_{k2}(t), t_{k2})$ defined in (A.13). For boundary constraints in $q_{k2}(t)$, we have

$$q_{k2}(t_{k2}) = H - h_k, v_{k2}(0) = v_{k2}(t_{k2}) = 0. \qquad (2)$$

By substituting $q(t) = 0$ and $T_0 = t_{k3}$ into (A.8), the hover energy consumption in the third step is $E_3(t_{k3}) = (P_0 + P_1)t_{k3}$. In the fourth step, the vertical climb energy can be given by $E_4(q_{k4}(t), t_{k4})$ defined in (A.15). For boundary constraints in $q_{k4}(t)$, we also have

$$q_{k4}(t_{k4}) = H - h_k, v_{k4}(0) = v_{k4}(t_{k4}) = 0. \qquad (3)$$

The total energy consumption of the UAV includes two components: the communication-related energy due to radiation, signal processing and other circuit, and the propulsion energy for ensuring the UAV to remain aloft. In practice, the propulsion energy is much larger than the communication-related energy which can therefore be ignored [39] in this paper. Thus, the total energy consumption of the UAV in the k-th ($k \le K$) stage is

$$E_k^{\text{Tot}} = \sum_{s \in \mathcal{S}} E_s(q_{ks}(t), t_{ks}) + (P_0 + P_1)t_{k3}, \qquad (4)$$

where $\mathcal{S} = \{1, 2, 4\}$.

For the $(K+1)$-th stage, the UAV flies from A_K back to the initial point A_0 with trajectory $q_{(K+1)1}(t)$ and time duration $t_{(K+1)1}$. As a result, the total energy consumption of the UAV in the $(K + 1)$-th stage amounts to

$$E_{K+1}^{\text{Tot}} = E_1(q_{(K+1)1}(t), t_{(K+1)1}). \qquad (5)$$

For boundary constraints in $q_{K+1}(t)$, we have

$$q_{(K+1)1}(t_{K+1}) = d_{\pi_K \pi_{K+1}}, v_{K+1}(0) = v_{K+1}(t_{(K+1)1}) = 0, \qquad (6)$$

where we denote $\pi_{K+1} = 0$.

For the third step in the k-th stage ($k \le K$) with staying stably at point O_k, the UAV broadcasts energy and receives information in HD or FD mode.

1) HD Mode: In HD mode, the UAV broadcasts energy to user k with power P in time duration $\rho_k t_{k3}$, and then user k utilizes the harvested energy to upload a fixed amount of data to the UAV in time duration $(1 - \rho_k)t_{k3}$, where $\rho_k \in [0, 1]$ is the time splitting factor for user π_k.

For UAV-ground links, large-scale attenuation is usually modelled as a random variable depending on the occurrence probabilities of LoS and non-LoS. The UAV is equipped with directional antenna. The channel gain between the UAV at point O_k and user π_k is denoted by g_k, which can be expressed as [25], [29], [46]

$$g_k = \begin{cases} \sqrt{\beta_0 h_k^{-\alpha}} z_k, & \text{with probability } a, \\ \sqrt{\kappa \beta_0 h_k^{-\alpha}} z_k, & \text{with probability } 1 - a. \end{cases} \qquad (7)$$

In (7), β_0 is channel power gain at the reference distance 1 m, α is the path loss exponent, κ is the additional attenuation factor due to the non-LoS condition, the small-scale fading z_k is exponentially distributed with parameter 1, and a is the LoS probability between the UAV and user π_k. In particular, a can be given by [25]

$$a = \frac{1}{1 + C_1(\exp(-C_2(90 - C_1)))}, \qquad (8)$$

where C_1 and C_2 are parameters depending on the propagation environment, and 90 is the elevation angle. The expected channel power gain by averaging over both randomness of small scaling fading and LoS occurrence is

$$\mathbb{E}(|g_k|^2) = (a + \kappa(1 - a))\beta_0 h_k^{-\alpha} = b h_k^{-\alpha}, \qquad (9)$$

where we set $b = (a + \kappa(1 - a))\beta_0$.

During the time duration of $\rho_k t_{k3}$, the harvested energy at user π_k can be evaluated by [40],

$$e_{\pi_k}^{\text{HD}} = \zeta P \rho_k t_{k3} \mathbb{E}(|g_k|^2) = \zeta P b h_k^{-\alpha} \rho_k t_{k3}, \qquad (10)$$

where $0 < \zeta < 1$ is the energy harvesting efficiency at user k.

During the time duration of $(1 - \rho_k)t_{k3}$ for uplink data transfer, the average transmit power of user π_k is p_{π_k}. Then, the transmitted data from user π_k to the UAV can be accordingly given by

$$d_{\pi_k}^{\text{HD}} = (1 - \rho_k)t_{k3}B \log_2\left(1 + \frac{p_k|g_k|^2}{B\sigma^2}\right), \qquad (11)$$

where B is the bandwidth of the system and σ^2 is the power spectral density of the additive white Gaussian noise. Due to the randomness of g_k, d_k^{HD} is a random variable. According to the Jensen's inequality, we have

$$\mathbb{E}(d_{\pi_k}^{\text{HD}}) \le (1 - \rho_k)t_{k3}B \log_2\left(1 + \frac{p_{\pi_k}\mathbb{E}(|g_k|^2)}{B\sigma^2}\right)$$
$$= (1 - \rho_k)t_{k3}B \log_2\left(1 + \frac{p_{\pi_k} b h_k^{-\alpha}}{B\sigma^2}\right) \triangleq r_{\pi_k}^{\text{HD}}. \qquad (12)$$

In the following, we use $r_{\pi_k}^{\text{HD}} \ge D_{\pi_k}$ to approximately represent the target data collection constraint, where D_{π_k} is the minimal required data of user π_k. Numerical results in [46] show rather satisfactory accuracy for such approximation.

Due to energy harvesting in time duration $\rho_k t_{k3}$ and data transmission in duration $(1 - \rho_k)t_{k3}$, the consumed energy at user π_k is

$$c_{\pi_k}^{\text{HD}} = \rho_k t_{k3} p_{\pi_k}^{\text{re}} + (1 - \rho_k)t_{k3}\left(p_{\pi_k}^{\text{tr}} + \frac{p_{\pi_k}}{\epsilon_{\pi_k}}\right), \qquad (13)$$

where $p_{\pi_k}^{\text{re}}$ is the receive circuit power consumption, $p_{\pi_k}^{\text{tr}}$ is the circuit power consumed for transmit signal processing, and $\epsilon_{\pi_k} \in (0, 1]$ is a constant which accounts for the power amplifier efficiency.

2) FD Mode: In FD mode, the UAV broadcasts energy to user π_k with power P, while user π_k simultaneously uploads the data to the UAV in time duration t_{k3} by using the harvested energy. The transmitted data from user π_k to the UAV in FD mode is

$$\mathbb{E}(d_{\pi_k}^{\text{FD}}) = \mathbb{E}\left((t_{k3} - \delta_{\pi_k})B\log_2\left(1 + \frac{p_{\pi_k}|g_k|^2}{\gamma P + B\sigma^2}\right)\right)$$
$$\leq (t_{k3} - \delta_{\pi_k})B\log_2\left(1 + \frac{p_{\pi_k}bh_k^{-\alpha}}{\gamma P + B\sigma^2}\right) \triangleq r_{\pi_k}^{\text{FD}}, \tag{14}$$

where γ denotes the effective self-interference coefficient in FD operations and δ_{π_k} is the processing delay of the energy circuits of user π_k. In time duration t_{k3}, the harvested energy at user π_k can be evaluated by [40],

$$e_{\pi_k}^{\text{FD}} = \zeta P b h_k^{-\alpha} t_{k3}, \qquad (15)$$

and the consumed energy at user π_k is

$$c_{\pi_k}^{\text{FD}} = t_{k3} p_{\pi_k}^{\text{re}} + (t_{k3} - \delta_{\pi_k})\left(p_{\pi_k}^{\text{tr}} + \frac{p_{\pi_k}}{\epsilon_{\pi_k}}\right). \qquad (16)$$

B. Problem Formulation

Now, it is ready to formulate the following total energy minimization problem with minimal user upload data demand as:

$$\min_{\boldsymbol{\pi},\boldsymbol{q},\boldsymbol{t},\boldsymbol{h},\boldsymbol{\rho},\boldsymbol{p}} \sum_{k=1}^{K+1} E_k^{\text{Tot}} \tag{17a}$$

$$\text{s.t.} \quad r_{\pi_k}^{\text{HD}} \geq D_{\pi_k}, \forall k \in \mathcal{K} \tag{17b}$$

$$e_{\pi_k}^{\text{HD}} \geq c_{\pi_k}^{\text{HD}}, \forall k \in \mathcal{K} \tag{17c}$$

$$0 \leq \rho_k \leq 1, \forall k \in \mathcal{K} \tag{17d}$$

$$q_{ks}(0) = q_{(K+1)1}(0) = 0, \forall k \in \mathcal{K}, s \in \mathcal{S} \tag{17e}$$

$$q_{k1}(t_{k1}) = d_{\pi_{k-1}\pi_k}, \forall k \in \mathcal{K}' \tag{17f}$$

$$q_{ks}(t_{ks}) = H - h_k, \forall k \in \mathcal{K}, s = 2, 4 \tag{17g}$$

$$v_{k1}(0) = v_{k1}(t_{k1}) = 0, \forall k \in \mathcal{K}' \tag{17h}$$

$$v_{ks}(0) = v_{ks}(t_{ks}) = 0, \forall k \in \mathcal{K}, s = 2, 4 \tag{17i}$$

$$v_{ks}(t) = \dot{q}_{ks}(t), a_{ks}(t) = \ddot{q}_{ks}(t), \forall k \in \mathcal{K}, s = 2, 4 \tag{17j}$$

$$v_{k1}(t) = \dot{q}_{k1}(t), a_{k1}(t) = \ddot{q}_{k1}(t), \forall k \in \mathcal{K}' \tag{17k}$$

$$|v_{ks}(t)| \leq V_{\max}, |a_{ks}(t)| \leq A_{\max}, \forall k \in \mathcal{K}', s \in \mathcal{S} \tag{17l}$$

$$\boldsymbol{\pi} \in \Pi \tag{17m}$$

for HD, and

$$\min_{\boldsymbol{\pi},\boldsymbol{q},\boldsymbol{t},\boldsymbol{h},\boldsymbol{p}} \sum_{l=1}^{K+1} E_l^{\text{Tot}} \tag{18a}$$

$$\text{s.t.} \quad r_{\pi_k}^{\text{FD}} \geq D_{\pi_k}, \forall k \in \mathcal{K} \tag{18b}$$

$$e_{\pi_k}^{\text{FD}} \geq c_{\pi_k}^{\text{FD}}, \forall k \in \mathcal{K} \tag{18c}$$

$$(17e) - (17m), \tag{18d}$$

for FD, where $\boldsymbol{\pi} = \{\pi_k\}$, $\boldsymbol{q} = \{q_{k1}(t), q_{k2}(t), q_{k4}(t)\}$, $\boldsymbol{t} = \{t_{k1}, t_{k2}, t_{k3}, t_{k4}\}$, $\boldsymbol{h} = \{h_k\}$, $\boldsymbol{\rho} = \{\rho_k\}$, $\boldsymbol{p} = \{p_k\}$, $\mathcal{K}' = \mathcal{K} \cup \{K + 1\}$, $V_{\max}$ and $A_{\max}$ are respectively the maximal velocity and acceleration of the UAV, and Π is the set of all possible permutation of all K users. Constraints (17b) or (18b) ensure successful data collection, while constraints (17c) or (18c) mean that the consumed energy of each user should be less than the harvested energy. The time splitting factor constraints are given in (17d). Constraints (17e)-(17i) are the boundary constraints for the trajectory.

Note that the trajectory from A_k to O_k always exists since the data from all users should be collected. Moreover, the discrete data collecting order variable $\boldsymbol{\pi}$ only affects the boundary constraints of fist-step trajectory in each fly-hover-communicate stage. This motivates us to decouple the energy minimization problem with two subproblems without loss of generality, i.e., path planning subproblem with variable $(\boldsymbol{\pi}, \bar{\boldsymbol{q}} = \{q_{k1}(t)\}, \bar{\boldsymbol{t}} = \{t_{k1}\})$ and energy minimization subproblem with variable $(\tilde{\boldsymbol{q}} = \{q_{k2}(t), q_{k4}(t)\}, \tilde{\boldsymbol{t}} = \{t_{k2}, t_{k3}, t_{k4}\}, \boldsymbol{h}, \boldsymbol{\rho}, \boldsymbol{p})$ for HD mode and $(\tilde{\boldsymbol{q}}, \tilde{\boldsymbol{t}}, \boldsymbol{h}, \boldsymbol{p})$ for FD mode.

III. PATH PLANNING

In this section, the path planning problem is investigated. According to (4), (5), problems (17) and (18), the path planning subproblem can be formulated as

$$\min_{\boldsymbol{\pi},\bar{\boldsymbol{q}},\bar{\boldsymbol{t}}} \sum_{k=1}^{K+1} E_1(q_{k1}(t), t_{k1}) \tag{19a}$$

$$\text{s.t.} \quad q_{k1}(0) = 0, q_{k1}(t_{k1}) = d_{\pi_{k-1}\pi_k}, \forall k \in \mathcal{K}' \tag{19b}$$

$$v_{k1}(0) = v_{k1}(t_{k1}) = 0, \forall k \in \mathcal{K}' \tag{19c}$$

$$v_{k1}(t) = \dot{q}_{k1}(t), a_{k1}(t) = \ddot{q}_{k1}(t), \forall k \in \mathcal{K}' \tag{19d}$$

$$|v_{k1}(t)| \leq V_{\max}, |a_{k1}(t)| \leq A_{\max}, \forall k \in \mathcal{K}' \tag{19e}$$

$$\boldsymbol{\pi} \in \Pi. \tag{19f}$$

Based on (19b), it is observed that the trajectory is a function of $d_{\pi_k\pi_{k-1}}$. Due to this observation, problem (19) is further equivalent to

$$\min_{\boldsymbol{\pi}} \sum_{k=1}^{K+1} E_{\pi_{k-1}\pi_k} \tag{20a}$$

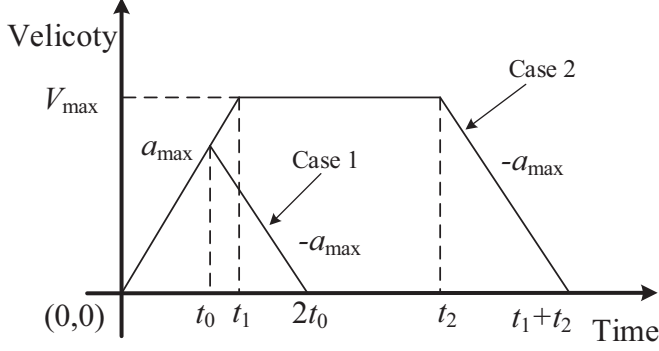$$\text{s.t.} \quad \boldsymbol{\pi} \in \Pi, \tag{20b}$$

Fig. 3. The velicoty versus time.

where

$$E_{\pi_k \pi_{k-1}} = \min_{q_{k1}(t), t_{k1}} E_1(q_{k1}(t), t_{k1}) \tag{21a}$$

$$\text{s.t.} \quad q_{k1}(0) = 0, q_{k1}(t_{k1}) = d_{\pi_{k-1}\pi_k} \tag{21b}$$

$$v_{k1}(0) = v_{k1}(t_{k1}) = 0 \tag{21c}$$

$$v_{k1}(t) = \dot{q}_{k1}(t), a_{k1}(t) = \ddot{q}_{k1}(t) \tag{21d}$$

$$|v_{k1}(t)| \le V_{\max}, |a_{k1}(t)| \le A_{\max}. \tag{21e}$$

In (21), $E_{\pi_{k-1}\pi_k}$ means the minimal propulsion energy consumption with flying distance $d_{\pi_{k-1}\pi_k}$.

For problem (21), in order to construct a feasible solution, we consider two special cases: 1) the UAV first increases the speed from zero to a specific speed less than $V_{\max}$ with the maximal acceleration $a_{\max}$ in time duration t_0, and then the UAV decreases the speed to zero with acceleration $-a_{\max}$; 2) the UAV first increases the speed from zero to $V_{\max}$ with acceleration $a_{\max}$ in time duration t_1, then the UAV flies with the constant speed, finally, the UAV decreases its speed to zero with acceleration $-a_{\max}$, as shown in Fig. 3. Constraints (21c)-(21e) can be easily satisfied if the UAV trajectory is determined. To satisfy constraint (21b), we consider the following two situations, separately.

1) If $d_{\pi_{k-1}\pi_k} < \frac{V_{\max}^2}{a_{\max}}$, the UAV trajectory follows case 1 in Fig. 3. In this case, we have $a_{\max}t_0^2 = d_{\pi_{k-1}\pi_k}$ and $t_{k1} = 2t_0$, i.e.,

$$t_{k1} = 2\sqrt{\frac{d_{\pi_{k-1}\pi_k}}{a_{\max}}}, \tag{22}$$

which implies that a feasible solution of (21) always exists.

2) If $d_{\pi_{k-1}\pi_k} \ge \frac{V_{\max}^2}{a_{\max}}$, the UAV trajectory follows case 2 in Fig. 3. In this case, we have $t_1 = \frac{V_{\max}}{a_{\max}}$, $\frac{V_{\max}^2}{a_{\max}} + (t_2 - t_1)V_{\max} = d_{\pi_{k-1}\pi_k}$ and $t_{k1} = t_1 + t_2$, i.e.,

$$t_{k1} = \frac{d_{\pi_{k-1}\pi_k}}{V_{\max}} + \frac{V_{\max}}{a_{\max}}, \tag{23}$$

which ensures a feasible solution of (21).

A. Solution for Problem (20)

To rewrite problem (20) in a simplifier manner, we introduce new variable w_{kl} to represent that the UAV collects data from user l in the k-th stage. With new variable $\boldsymbol{w} = \{w_{kl}\}$, problem (20) can be equivalently transformed to

$$\min_{\boldsymbol{w}} \quad \sum_{l=1}^{K} w_{1l}E_{0l} + \sum_{k=2}^{K}\sum_{l=1}^{K}\sum_{i=1}^{K} w_{(k-1)l}w_{ki}E_{li}$$

$$+ \sum_{l=1}^{K} w_{Kl}E_{l0} \tag{24a}$$

$$\text{s.t.} \quad \sum_{k=1}^{K} w_{kl} = 1, \forall l \in \mathcal{K} \tag{24b}$$

$$\sum_{l=1}^{K} w_{kl} = 1, \forall k \in \mathcal{K} \tag{24c}$$

$$w_{kl} \in \{0,1\}, \forall k, l \in \mathcal{K}. \tag{24d}$$

In the objective function (24a), $\sum_{l=1}^{K} w_{1l}E_{0l}$ means the energy consumption in the first stage. For $2 \le k \le K$, the term $w_{(k-1)l}w_{ki}E_{li}$ means the energy consumption in the k-th stage when the UAV visits user l in the $(k-1)$-th stage and visits user i in the k-th stage. Summing all possible cases, $\sum_{l=1}^{K}\sum_{i=1}^{K} w_{(k-1)l}w_{ki}E_{li}$ means the energy consumption in the k-th stage. The last term in (24a), $\sum_{l=1}^{K} w_{Kl}E_{l0}$ stands for the energy consumption in the last $(K+1)$-th stage since the UAV flies back to the initial point in this stage. Constraints (24b) represent that each user is visited at once, while constraints (24c) show that only one user is visited at each stage.

Problem (24) is a non-linear integer problem due to non-linear term $w_{(k-1)l}w_{ki}$ in the objective function. To transform problem (24) into an equivalent solvable form, we introduce new variable $v_{kli} = w_{(k-1)l}w_{ki}$. Due to the fact that $w_{kl} \in \{0,1\}$, constraint $v_{kli} = w_{(k-1)l}w_{ki}$ is equivalent to

$$v_{kli} \ge w_{(k-1)l} + w_{ki} - 1, v_{kli} \ge 0, \tag{25}$$

and

$$v_{kli} \le w_{(k-1)l}, v_{kli} \le w_{ki}, \tag{26}$$

for all $k = \mathcal{K} \setminus \{1\}$, $l, i \in \mathcal{K}$.

With new variable $\boldsymbol{v} = \{v_{kli}\}$, problem (24) is equivalent to the following integer problem

$$\min_{\boldsymbol{w}, \boldsymbol{v}} \quad \sum_{l=1}^{K} w_{1l}E_{0l} + \sum_{k=2}^{K}\sum_{l=1}^{K}\sum_{i=1}^{K} v_{kli}^2 E_{li}$$

$$+ \sum_{l=1}^{K} w_{Kl}E_{l0} \tag{27a}$$

$$\text{s.t.} \quad (24b) - (24d), (25), (26). \tag{27b}$$

Note that we use v_{kli}^2 to replace v_{kli} in the objective function (27a) because v_{kli} is always 0 or 1 according to (25) and (26). The advantage of transforming problem (24) into problem (27) is that problem (27) with relaxed constraints is convex.

Due to integer constraints (24d), it is hard to solve problem (27). By temporarily relaxing the integer constraints (24d) with

$w_{kl} \in [0,1]$, problem (27) is a convex problem. For convex problem (27) with relaxed constraints, the optimal solution can be effectively obtained by using the dual method [47], [48]. We show that it fortunately gets integer solutions, which preserves both optimality and feasibility of the original problem even though the relaxation is deployed temporarily.

To obtain the optimal solution of problem (27), we have the following theorem.

Theorem 1. *For problem (27), the optimal path planning $\boldsymbol{w}$ and auxiliary vector $\boldsymbol{v}$ can be respectively expressed as*

$$w_{kl}^* = \begin{cases} 1, & \text{if } k = \arg\min_{i \in \mathcal{K}} C_{il} \\ 0, & \text{otherwise,} \end{cases} \tag{28}$$

and

$$v_{kli}^* = \left[\frac{\gamma_{kli} - \lambda_{kli} - \mu_{kli}}{2E_{li}} \right]^+, \tag{29}$$

where

$$C_{kl} = \begin{cases} E_{0l} + \beta_1 + \sum_{i=1}^{K}(\gamma_{2li} - \lambda_{2li}), & \text{if } k = 1 \\ \beta_k + \sum_{i=1}^{K}(\gamma_{(k+1)li} + \gamma_{kil} - \lambda_{(k+1)li} - \mu_{kil}), & \\ & \quad \text{if } 2 \le k \le K-1 \\ E_{l0} + \sum_{i=1}^{K}(\gamma_{Kil} - \mu_{Kil}), & \text{if } k = K. \end{cases} \tag{30}$$

$\{\beta_k\}, \{\gamma_{kli}\}, \{\lambda_{kli}\}, \{\mu_{kli}\}$ *are Lagrange multipliers associated with corresponding constraints of problem (27), and $[x]^+ = \max\{x, 0\}$. If there are multiple minimal points in $\arg\min_{i \in \mathcal{K}} C_{il}$, we will choose any one of them.*

Proof. Please refer to Appendix B. □

The values of $\{\beta_k\}, \{\gamma_{kli}\}, \{\lambda_{kli}\}, \{\mu_{kli}\}$ can be determined by the sub-gradient method [49]. The updating procedure is given by

$$\beta_k = \beta_k + \phi\left(\sum_{l=1}^{K} w_{kl} - 1\right) \tag{31}$$

$$\gamma_{kli} = \left[\gamma_{kli} + \phi(w_{(k-1)l} + w_{ki} - 1 - v_{kli})\right]^+ \tag{32}$$

$$\lambda_{kli} = \left[\lambda_{kli} + \phi(v_{kli} - w_{(k-1)l})\right]^+ \tag{33}$$

$$\mu_{kli} = \left[\mu_{kli} + \phi(v_{kli} - w_{ki})\right]^+, \tag{34}$$

where $\phi > 0$ is a dynamically chosen step-size sequence.

By iteratively optimizing primal variable and dual variable, the optimal path planning is obtained. The dual method used to obtain the optimal path planning is given in Algorithm 1. Notice that the optimal w_{kl} is either 0 or 1 according to (28), even though we relax w_{kl} as continuous constraint in (27). Therefore, we can obtain optimal solution to problem (27).

Algorithm 1 Dual Method for Problem (27)

1: Initialize dual variables $\{\beta_k\}, \{\gamma_{kli}\}, \{\lambda_{kli}\}, \{\mu_{kli}\}$.
2: **repeat**
3:   Update path planning variable $\boldsymbol{w}$ and auxiliary vector $\boldsymbol{v}$ according to (28)-(30).
4:   Update dual variables based on (31)-(34).
5: **until** the objective value (27a) converges

For the complexity, according to Algorithm 1, the major complexity lies in updating $\boldsymbol{v}$. Based on (29), the complexity of calculating $\boldsymbol{v}$ is $\mathcal{O}(K^3)$. As a result, the total complexity of Algorithm 1 is $\mathcal{O}(LK^3)$, where L is the number of iterations in Algorithm 1.

B. Solution for Problem (21)

Problem (21) is difficult to be directly solved due to the following two difficulties. The first difficulty is the unknown fly time t_{k1}. The second difficulty is that problem (21) involves an infinite number of optimization variables in continuous-function $q_{k1}(t)$.

To handle the first difficulty, we provide the following lemma regarding the property about the optimal fly time. Denote the optimal solution of problem (21) by $(q_{k1}^*(t), t_{k1}^*)$.

Lemma 1. *With fixed fly time $t_{k1} > t_{k1}^*$, the optimal trajectory of problem (21) is*

$$\bar{q}_{kl}(t) = \begin{cases} q_{kl}^*(t), & \text{if } 0 \le t \le t_{k1}^* \\ q_{kl}^*(t_{k1}^*), & \text{if } t_{k1}^* \le t \le t_{k1}. \end{cases} \tag{35}$$

Proof. According to (A.6), it is observed that the propulsion power of the UAV with positive velocity is strictly larger than the propulsion power $P_0 + P_1$ with zero velocity (i.e., the UAV is stable). Since $q_{k1}^*(t)$ is the optimal solution for problem (21) with fixed optimal fly t_{k1}^*, the optimal $\bar{q}_{kl}(t)$ of roblem (21) with $t_{k1} > t_{k1}^*$ should be given by (35). □

Based on Lemma 1, it is observed that the optimal solution of problem (21) can be constructed by solving problem (21) even with fixed fly time $(t_{k1} > t_{k1}^*)$. For the upper bound of the optimal fly time, the following lemma is provided.

Lemma 2. *Given a feasible solution of problem (21) with objective value E, the optimal fly time t_{k1}^* of problem (21) satisfies $t_{k1}^* < \frac{E}{P_0+P_1}$.*

Proof. Denote E^* as the optimal objective value of problem (21). Then, we have $E^* \le E$. Due to the fact that the propulsion power of the UAV with positive velocity is strictly larger than $P_0 + P_1$ according to (A.6), we can obtain that $E^* > (P_0 + P_1)t_{k1}^*$. Thus, we have $t_{k1}^* < \frac{E}{P_0+P_1}$. □

Based on Lemma 1, problem (21) can be effectively solved without loss of optimality even with fixed fly time obtained from Lemma 2.

To handle the second difficulty, problem (21) can be reformulated with applying discrete linear state-space approximation. By discretizing the time duration t_{k1} into $N+1$ slots with step size $\delta = \frac{t_{k1}}{N}$, i.e., $t = n\delta$, $n = 0, 1, \cdots, N$, the UAV trajectory $q_{k1}(t)$ can be characterized by the discrete-time UAV location $\{q_{k1n}\}$. For continuous constraints (21d) with small step size δ, we have the following equation about the velocity $\{v_{k1n}\}$ and acceleration $\{a_{k1n}\}$

$$v_{k1n} = \frac{q_{k1n} - q_{k1(n-1)}}{\delta}, \forall n \in \mathcal{N} \tag{36}$$

$$a_{k1n} = \frac{v_{k1n} - v_{k1(n-1)}}{\delta}, \forall n \in \mathcal{N}, \tag{37}$$

where $\mathcal{N} = \{1, \cdots, N\}$. The maximal velocity and acceleration constraints (21e) can be accordingly presented as

$$|v_{k1n}| \le V_{\max}, |a_{k1n}| \le A_{\max}, \forall n \in \mathcal{N}. \tag{38}$$

As a result, problem (21) can be expressed in the discrete form as

$$\min_{\{q_{k1n}\},\{v_{k1n}\},\{a_{k1n}\}} \bar{E}_1(\{q_{k1n}\},\{v_{k1n}\},\{a_{k1n}\}) \tag{39a}$$

$$\text{s.t.} \quad q_{k10}=0, q_{k1N}=d_{\pi_{k-1}\pi_k} \tag{39b}$$

$$v_{k10}=v_{k1N}=0 \tag{39c}$$

$$(36)-(38), \tag{39d}$$

where

$$\bar{E}_1(\{q_{k1n}\},\{v_{k1n}\},\{a_{k1n}\}) = \sum_{n=1}^{N}\Bigg[P_0\left(1+c_1 v_{k1n}^2\right)$$
$$+ P_1 \sqrt{1+(c_2 v_{k1n}^2 + c_3 a_{k1n} v_{k1n})^2}$$
$$\times \sqrt{\sqrt{1+(c_2 v_{k1n}^2 + c_3 a_{k1n} v_{k1n})^2 + c_4^2 v_{k1n}^4} - c_4 v_{k1n}^2}$$
$$+ c_5 v_{k1n}^3 \Bigg]. \tag{40}$$

Equation (40) is derived from (A.8).

Problem (39) is non-convex due to the objective function (40). It is generally hard to find the globally optimal solution of non-convex problem (39). In the following, we use the successive convex approximation (SCA) technique to obtain a suboptimal solution.

The second term in (40) is non-convex. To handle this issue, we introduce slack variables A_n and B_n such that

$$A_n = c_2 v_{k1n}^2 + c_3 a_{k1n} v_{k1n}, \tag{41}$$

and

$$B_n = \sqrt{\sqrt{1+A_n^2 + c_4^2 v_{k1n}^4} + c_4 v_{k1n}^2}. \tag{42}$$

Therefore, the second term in (40) can be replaced by the convex expression $\frac{1+A_n^2}{B_n}$. With the above manipulations, problem (39) can be equivalent to

$$\min_{\substack{\{q_{k1n}\},\{v_{k1n}\},\\ \{a_{k1n}\},\{A_n\},\{B_n\}}} \sum_{n=1}^{N}\left[P_0\big(1+c_1 v_{k1n}^2\big)+\frac{P_1(1+A_n^2)}{B_n}+c_5 v_{k1n}^3\right] \tag{43a}$$

$$\text{s.t.} \quad A_n \geq c_2 v_{k1n}^2 + c_3 a_{k1n} v_{k1n}, \forall n \in \mathcal{N} \tag{43b}$$

$$B_n^2 \leq \sqrt{1+A_n^2 + c_4^2 v_{k1n}^4} + c_4 v_{k1n}^2, \forall n \in \mathcal{N} \tag{43c}$$

$$B_n \geq 0, \forall n \in \mathcal{N} \tag{43d}$$

$$(39b)-(39c),(36)-(38). \tag{43e}$$

Note that the constraints (43b) and (43c) are obtained from (41) and (42) by replacing the equalities with inequalities. The reason is that for the optimal solution of problem (43), constraints (43b) and (43c) always hold with equality.

Algorithm 2 SCA-Based Algorithm for Problem (43)

1: Obtain a feasible $(\{q_{k1n}^{(0)}\},\{v_{k1n}^{(0)}\},\{a_{k1n}^{(0)}\},\{A_n^{(0)}\},\{B_n^{(0)}\})$ of problem (43). Set $j=0$.
2: **repeat**
3:      Replace $a_{k1n}v_{k1n}$ in (43b) with $r_{1n}^{(j)}(a_{k1n},v_{k1n})$ and the right hand side of (43c) with $r_{2n}^{(j)}(A_n,v_{k1n})$.
4:      Obtain the optimal $(\{q_{k1n}^{(j+1)}\},\{v_{k1n}^{(j+1)}\},\{a_{k1n}^{(j+1)}\},\{A_n^{(j+1)}\},\{B_n^{(j+1)}\})$ of convex problem (43).
5:      Set $j=j+1$.
6: **until** the objective value (43a) converges.

Problem (43) is still non-convex due to the introduced non-convex constraints (43b) and (43c). For the non-convex term $a_{k1n}v_{k1n}$ in constraints (43b), we have

$$a_{k1n}v_{k1n} = \frac{1}{4}[(a_{k1n}+v_{k1n})^2 - (a_{k1n}-v_{k1n})^2]$$
$$\leq \frac{1}{4}[(a_{k1n}+v_{k1n})^2 - 2(a_{k1n}^{(j)}-v_{k1n}^{(j)})$$
$$\times (a_{k1n}-a_{k1n}^{(j)}+v_{k1n}-v_{k1n}^{(j)}) - (a_{k1n}^{(j)}-v_{k1n}^{(j)})^2]$$
$$\triangleq r_{1n}^{(j)}(a_{k1n},v_{k1n}), \tag{44}$$

where the superscript (j) means the value of variable at the j-th iteration and the inequality follows from the fact that a convex function is no less than its first-order Taylor expansion.

Through analyzing all the principal minors of Hessian matrix, $\sqrt{1+A_n^2 + c_4^2 v_{k1n}^4}$ is a convex function of variable (A_n, v_{k1n}). For the right hand side of constraints (43c), we can obtain

$$\sqrt{1+A_n^2+c_4^2 v_{k1n}^4}+c_4 v_{k1n}^2 \geq (1+(A_n^{(j)})^2+c_4^2(v_{k1n}^{(j)})^4)^{-\frac{1}{2}}$$
$$\times [A_n^{(j)}(A_n - A_n^{(j)}) + 2c_4^2(v_{k1n}^{(j)})^3(v_{k1n}-v_{k1n}^{(j)})]$$
$$+ \sqrt{1+(A_n^{(j)})^2+c_4^2(v_{k1n}^{(j)})^4}+c_4(v_{k1n}^{(j)})^2$$
$$+ 2c_4(v_{k1n}-v_{k1n}^{(j)}) \triangleq r_{2n}^{(j)}(A_n,v_{k1n}). \tag{45}$$

By replacing the term $a_{k1n}v_{k1n}$ in (43b) with its upper bound $r_{1n}^{(j)}(a_{k1n},v_{k1n})$ and the right hand side of constraints (43c) with the lower bound $r_{2n}^{(j)}(A_n,v_{k1n})$, problem (43) becomes a convex problem, which can be effectively solved by the interior point method [47]. The SCA-based algorithm for problem (43) is summarized in Algorithm 2.

IV. ENERGY MINIMIZATION WITH FIXED PATH PLANNING

In this section, the energy minimization problems for HD and FD modes with optimal path planning are respectively solved. According to problems (17) and (18), the energy

minimization with fixed path planning can be formulated as

$$\min_{\tilde{\boldsymbol{q}},\tilde{\boldsymbol{t}},\boldsymbol{h},\boldsymbol{\rho},\boldsymbol{p}} \sum_{k=1}^{K} [E_2(q_{k2}(t),t_{k2}) + E_4(q_{k4}(t),t_{k4}) + (P_0+P_1)t_{k3}]$$

(46a)

$$\text{s.t.} \quad r_{\pi_k}^{\text{HD}} \geq D_{\pi_k}, \forall k \in \mathcal{K} \tag{46b}$$

$$e_{\pi_k}^{\text{HD}} \geq c_{\pi_k}^{\text{HD}}, \forall k \in \mathcal{K} \tag{46c}$$

$$0 \leq \rho_k \leq 1, \forall k \in \mathcal{K} \tag{46d}$$

$$q_{ks}(0) = 0, q_{ks}(t_{ks}) = H - h_k, \forall k \in \mathcal{K}, s = 2,4 \tag{46e}$$

$$v_{ks}(0) = v_{ks}(t_{ks}) = 0, \forall k \in \mathcal{K}, s = 2,4 \tag{46f}$$

$$v_{ks}(t) = \dot{q}_{ks}(t), a_{ks}(t) = \ddot{q}_{ks}(t), \forall k \in \mathcal{K}, s = 2,4 \tag{46g}$$

$$|v_{ks}(t)| \leq V_{\max}, |a_{ks}(t)| \leq A_{\max}, \forall k \in \mathcal{K}, s = 2,4, \tag{46h}$$

for HD, and

$$\min_{\tilde{\boldsymbol{q}},\tilde{\boldsymbol{t}},\boldsymbol{h},\boldsymbol{p}} \sum_{k=1}^{K} [E_2(q_{k2}(t),t_{k2}) + E_4(q_{k4}(t),t_{k4}) + (P_0+P_1)t_{k3}]$$

(47a)

$$\text{s.t.} \quad r_{\pi_k}^{\text{FD}} \geq D_{\pi_k}, \forall k \in \mathcal{K} \tag{47b}$$

$$e_{\pi_k}^{\text{FD}} \geq c_{\pi_k}^{\text{HD}}, \forall k \in \mathcal{K} \tag{47c}$$

$$(46e) - (46h), \tag{47d}$$

for FD.

From (46) and (47), both objective function and constraints can be decoupled for k. Thus, it reduces to solve the specific energy minimization problem for a specific user in steps 2-4 of each stage. It is also observed that with fixed h_k the energy consumption $E_2(q_{k2}(t),t_{k2}) + E_4(q_{k4}(t),t_{k4})$ is independent of energy consumption $(P_0+P_1)t_{k3}$. Based on the above observations, problem (46) for a specific k can be equivalent to

$$\min_{h_k} = V_1(h_k) + V_2(h_k), \tag{48}$$

where $V_1(h_k)$ is the optimal objective value of problem (49) given as

$$\min_{\substack{q_{k2}(t),q_{k4}(t), \\ t_{k2},t_{k4}}} E_2(q_{k2}(t),t_{k2}) + E_4(q_{k4}(t),t_{k4}) \tag{49a}$$

$$\text{s.t.} \quad q_{ks}(0) = 0, q_{ks}(t_{ks}) = H - h_k, \forall s = 2,4 \tag{49b}$$

$$v_{ks}(0) = v_{ks}(t_{ks}) = 0, \forall s = 2,4 \tag{49c}$$

$$v_{ks}(t) = \dot{q}_{ks}(t), a_{ks}(t) = \ddot{q}_{ks}(t), \forall s = 2,4 \tag{49d}$$

$$|v_{ks}(t)| \leq V_{\max}, |a_{ks}(t)| \leq A_{\max}, \forall s = 2,4, \tag{49e}$$

and $V_2(h_k)$ is the optimal objective value of problem (50) given as

$$\min_{t_{k3},\rho_k,p_{\pi_k}} (P_0+P_1)t_{k3} \tag{50a}$$

$$\text{s.t.} \quad (1-\rho_k)t_{k3}B\log_2\left(1 + \frac{p_{\pi_k}bh_k^{-\alpha}}{B\sigma^2}\right) \geq D_{\pi_k} \tag{50b}$$

$$\zeta P b h_k^{-\alpha}\rho_k t_{k3} \geq \rho_k t_{k3} p_{\pi_k}^{\text{re}}$$
$$+ (1-\rho_k)t_{k3}\left(p_{\pi_k}^{\text{tr}} + \frac{p_{\pi_k}}{\epsilon_{\pi_k}}\right) \tag{50c}$$

$$0 \leq \rho_k \leq 1. \tag{50d}$$

Note that we have substituted the value of $r_{\pi_k}^{\text{FD}}, e_{\pi_k}^{\text{FD}}, c_{\pi_k}^{\text{HD}}$ into problem (50) according to (10)-(13). Similarly, problem (47) with a fixed k can be equivalent to

$$\min_{h_k} = V_1(h_k) + V_3(h_k), \tag{51}$$

where $V_3(h_k)$ is the optimal objective value of problem (52) given as

$$\min_{t_{k3},p_{\pi_k}} (P_0+P_1)t_{k3} \tag{52a}$$

$$\text{s.t.} \quad (t_{k3} - \delta_{\pi_k})B\log_2\left(1 + \frac{p_{\pi_k}bh_k^{-\alpha}}{\gamma P + B\sigma^2}\right) \geq D_{\pi_k} \tag{52b}$$

$$\zeta P b h_k^{-\alpha} t_{k3} \geq t_{k3}p_{\pi_k}^{\text{re}} + (t_{k3} - \delta_{\pi_k})\left(p_{\pi_k}^{\text{tr}} + \frac{p_{\pi_k}}{\epsilon_{\pi_k}}\right). \tag{52c}$$

Since problems (48) and (51) only involve only one variable, the 1D exhaustive search method can be used to obtain the optimal solution. In the following, we separately solve problems (49), (50), and (52).

For the feasibility of problem (49), the feasible solution can be obtained as in (22) and (23). For problems (50) and (52), the optimal solutions are obtained in closed form according to the following Theorems 2 and 3.

A. Vertical Trajectory Optimization for Problem (49)

According to Lemmas 1 and 2 in Section III-B, problem (49) can be effectively solved without loss of optimality even with fixed t_{k2} and t_{k4}. Similar to Section III-B, the discrete linear state-space approximation is adopted. By discretizing the time duration t_{k2} (t_{k4}) into $N+1$ slots with step size $\delta_2 = \frac{t_{k2}}{N_2}$ ($\delta_4 = \frac{t_{k4}}{N_4}$), i.e., $t = n\delta_2$ ($t = n\delta_4$), $n = 0,1,\cdots,N$, the UAV trajectory $q_{k2}(t)$ ($q_{k4}(t)$) can be characterized by the discrete-time UAV location $\{q_{k4n}\}$ ($\{q_{k4n}\}$). As a result, problem (49) can be expressed in the discrete form as

$$\min_{\substack{\{q_{k2n}\},\{v_{k2n}\},\{a_{k2n}\}, \\ \{q_{k4n}\},\{v_{k4n}\},\{a_{k4n}\}}} P_2(t_{k2}+t_{k4}) + Wh_k$$

$$+ \sum_{n=1}^{N} \frac{W - ma_{k2n}}{2}\sqrt{v_{k2n}^2 + \frac{2(W - ma_{k2n})}{\rho A}}$$

$$+ \sum_{n=1}^{N} \frac{W + ma_{k4n}}{2}\sqrt{v_{k4n}^2 + \frac{2(W + ma_{k4n})}{\rho A}} \tag{53a}$$

$$\text{s.t.} \quad q_{ks0} = 0, q_{ksN} = H - h_k, \forall s = 2,4 \tag{53b}$$

$$v_{ks0} = v_{ksN} = 0, \forall s = 2,4 \tag{53c}$$

$$(36) - (38), \tag{53d}$$

The formulation of objective function (53a) comes from (A.13) and (A.15).

Problem (53) is non-convex due to non-convex objective function (53a). To handle this issue, we introduce variables X_n and Y_n such that

$$X_n = \sqrt{v_{k2n}^2 + \frac{2(W - ma_{k2n})}{\rho A}}, \tag{54}$$

and

$$Y_n = \sqrt{v_{k4n}^2 + \frac{2(W + ma_{k4n})}{\rho A}}. \quad (55)$$

With the above manipulations, problem (53) can be equivalent to

$$\min_{\substack{\{q_{k2n}\},\{v_{k2n}\},\{a_{k2n}\}, \\ \{q_{k4n}\},\{v_{k4n}\},\{a_{k4n}\}, \\ \{X_n\},\{Y_n\}}} P_2(t_{k2} + t_{k4}) + Wh_k$$

$$+ \sum_{n=1}^{N} \frac{WX_n - ma_{k2n}X_n + WY_n + ma_{k4n}Y_n}{2}$$

$$(56a)$$

$$\text{s.t.} \quad X_n^2 \geq v_{k2n}^2 + \frac{2(W - ma_{k2n})}{\rho A} \quad (56b)$$

$$Y_n^2 \geq v_{k4n}^2 + \frac{2(W + ma_{k4n})}{\rho A} \quad (56c)$$

$$(53b), (53c), (36) - (38). \quad (56d)$$

Note that the constraints (56b) and (56c) are obtained from (54) and (55) by replacing the equalities with inequalities. To handle the non-convexity of $-a_{k2n}X_n + a_{k4n}Y_n$ in (43a), the convex approximation can be obtained by using the similar method in (44). Moreover, for the left hand sides of (56b) and (56c) can be approximated by its first-order Taylor expansion as in (45). As a result, problem (56) can be solved by the SCA-based algorithm.

B. HD Mode for Problem (50)

Theorem 2. *For HD, the optimal solution of problem* (50), $(t_{k3}^*, \rho_k^*, p_{\pi_k}^*)$, *is given by*

$$t_{k3}^* = t_{k31}^* + t_{k32}^*, \quad \rho_k^* = \frac{t_{k31}^*}{t_{k31}^* + t_{k32}^*}, \quad (57)$$

and

$$p_{\pi_k}^* = \frac{\epsilon_{\pi_k}(\zeta Pbh_k^{-\alpha} - p_{\pi_k}^{re})t_{k31}^*}{t_{k32}^*} - \epsilon_{\pi_k}p_{\pi_k}^{tr} \cdot, \quad (58)$$

where

$$t_{k31}^* = \left(2^{\frac{D}{Bt_{k32}^*}} - u_1\right)\frac{t_{k32}^*}{u_2}. \quad (59)$$

$$t_{k32}^* = \frac{(\ln 2)D}{BW\left(\frac{u_2-1}{e}\right) + B}, \quad (60)$$

$$u_1 = 1 - \frac{\epsilon_{\pi_k}p_{\pi_k}^{tr}bh_k^{-\alpha}}{B\sigma^2}, u_2 = \frac{\epsilon_{\pi_k}(\zeta Pbh_k^{-\alpha} - p_{\pi_k}^{re})bh_k^{-\alpha}}{B\sigma^2}. \quad (61)$$

and $W(\cdot)$ *is the Lambert-W function.*

Proof. Please refer to Appendix C. □

According to Theorem 1, the optimal solution of problem (50) for HD is obtained in closed form. Based on (61), we must have $\zeta Pbh_k^{-\alpha} - p_{\pi_k}^{re} > 0$, which means that the harvested power at user π_k must be greater than its receive power, i.e., the following constraint about the UAV hight is obtained

$$h_k < \left(\frac{\zeta Pb}{p_{\pi_k}^{re}}\right)^{\frac{1}{\alpha}}. \quad (62)$$

C. FD Mode for Problem (52)

Theorem 3. *For FD, the optimal solution of problem* (52), $(t_{k3}^*, p_{\pi_k}^*)$, *satisfies,* t_{k3}^* *is the solution to the following equation*

$$\left(2^{\frac{D}{B(t_{k3} - \delta_{\pi_k})}} - 1\right)\frac{\gamma P + B\sigma^2}{bh_k^{-\alpha}} - \frac{\epsilon_{\pi_k}(\zeta Pbh_k^{-\alpha} - p_{\pi_k}^{re})t_{k3}}{t_{k3} - \delta_{\pi_k}}$$

$$+ \epsilon_{\pi_k}p_{\pi_k}^{tr} = 0. \quad (63)$$

and

$$p_{\pi_k}^* = \left(2^{\frac{D}{B(t_{k3}^* - \delta_{\pi_k})}} - 1\right)\frac{\gamma P + B\sigma^2}{bh_k^{-\alpha}}. \quad (64)$$

Proof. Please refer to Appendix D. □

Since the left hand side of equation (63) is monotonically decreasing with t_{k3}, the unique solution t_{k3}^* to (63) can be obtained by the bisection method. For the case that $\delta_k \approx 0$, to ensure $p_{\pi_k} > 0$ from (52c), we must have

$$h_k < \left(\frac{\zeta Pb}{p_{\pi_k}^{re} + p_{\pi_k}^{tr}}\right)^{\frac{1}{\alpha}}. \quad (65)$$

V. NUMERICAL RESULTS

There are $K = 8$ users uniformly in a square area of size 1000 m $\times$ 1000 m with the UAV initially located at its center. The noise power spectrum density is $\sigma^2 = -174$ dBm/Hz. We set reference channel gain $\beta_0 = 1.42 \times 10^{-4}$ [50] and energy harvesting coefficient $\zeta = 0.9$. The maximal flying speed of the UAV is $V_{\max} = 30$ m/s and the maximal acceleration is $A_{\max} = 5$ m/s^2. All users have the same power amplifier efficiency $\epsilon_k = 0.9$, the same processing delay of the energy circuits $\delta_k = 2$ s, and the same minimal required data $D_k = D$. The modeling coefficients for the probabilistic LoS channel model are set as $C_1 = 10$, $C_2 = 0.6$, $\kappa = 0.2$, and $\alpha = 2.3$. Unless specified otherwise, the system parameters are set as: the UAV altitude is $H = 120$ m, the maximal wireless transmission power of the UAV is $P = 1$ W, the system bandwidth is $B = 20$ MHz, the receive and transmit circuit power consumption are respectively set as $p_k^{re} = p^{re} = 1$ uW and $p_k^{tr} = p^{tr} = 1$ mW for all users, the self-interference coefficient $\gamma = -100$ dBm, and the minimal required data is $D = 1$ Mbits.

The total energy consumption versus UAV altitude H is illustrated in Fig. 4. We compare the proposed optimal path planning Algorithm 1 (labeled as 'Proposed'), with the exhaustive search method to obtain the optimal path planning (labeled as 'Exhaustive'), and the random method to obtain a feasible path planning (labeled as 'Random'). It is found that the proposed algorithm achieves the same performance as the exhaustive search method, which shows the optimality of the proposed algorithm. From this figure, it is also shown that the total energy consumption linearly increases with altitude H. This is because high altitude means long distance the UAV needs to change for energy broadcast and information reception, which results high propulsion energy consumption of the UAV.

In Fig. 5, we illustrate the optimal height h_k in problems (48) and (51) versus minimal required data D. From this
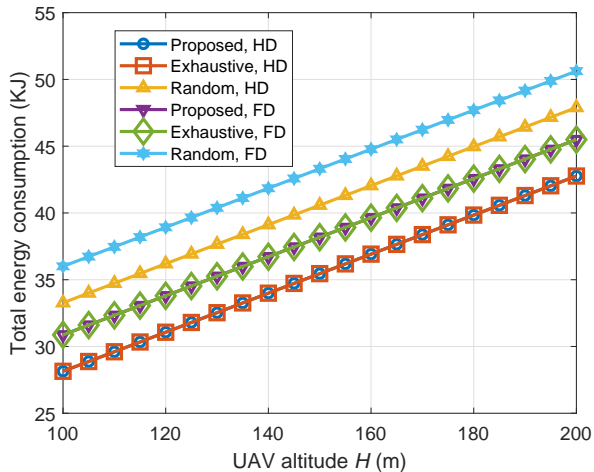
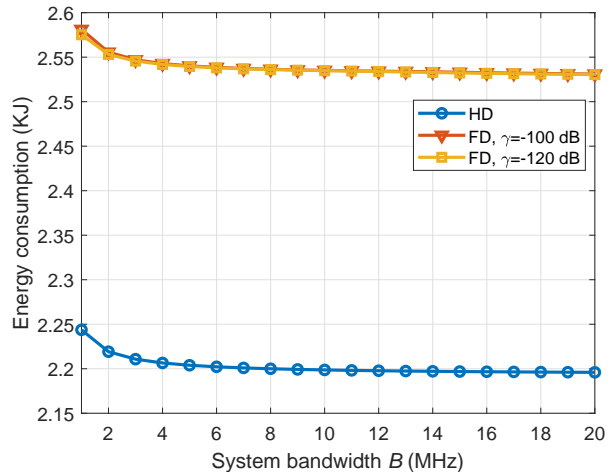Fig. 4. Total energy consumption versus UAV altitude H.

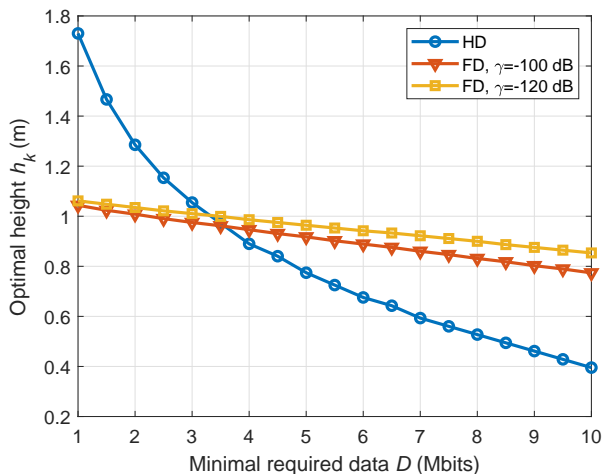Fig. 6. Energy consumption versus system bandwidth with $D = 10$ Mbits.

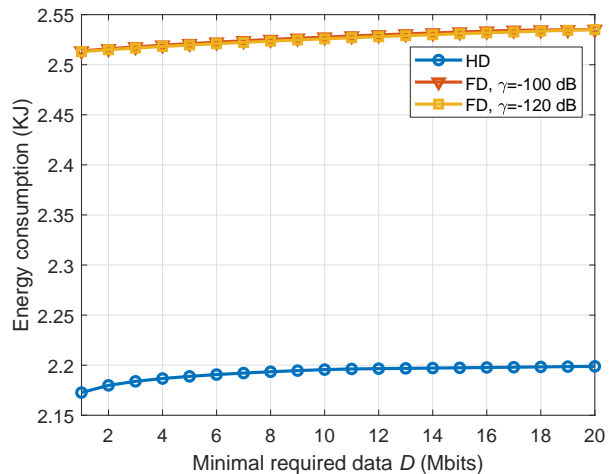Fig. 5. Optimal height versus minimal required data D.

Fig. 7. Energy consumption versus minimal required data D.

figure, it is found that the optimal height decreases with an increasing D. This is due to the fact that high minimal required data needs high data rate to decrease the transmission time, while low height can lead to high data rate between the user and the UAV. It is also found that the decrease speed of the optimal height for HD is higher than that for FD. For low data demand, i.e., $D \leq 3$ Mbits, the optimal hight of HD is higher than that of FD. As for high data demand, i.e., $D > 3$ Mbits, the optimal hight of HD is lower than that of FD. According to this figure, it is observed that the optimal hight is low, less than 2 m. The reason is that the channel gain is the better for small hight, which results in short staying time and low energy consumption.

The energy consumption in the following Figs. 6 to 8 means the energy consumption in (48a) and (51a), which includes the energy for the UAV to firstly decrease the altitude, then collect data and finally increase the altitude. Fig. 6 presents the energy consumption versus system bandwidth. From this figure, it is shown that the energy consumption first decreases rapidly with bandwidth and then decreases slowly with bandwidth.

This is because for small bandwidth, the UAV hovering time is long and the propulsion energy during hovering decreases rapidly with the increase of bandwidth. For high bandwidth, the hovering time is short and thus the propulsion energy for the UAV to change height dominates the energy consumption.

The total energy consumption versus minimal data demand D is depicted in Fig. 7. It can be observed that the total energy consumption monotonically increases with minimal data demand. This is because high minimal data demand leads to long hovering time of the UAV, which increases the energy consumption of the UAV. It is also found that the HD is always superior over FD, and FD with low self-interference coefficient, i.e., $\gamma = -120$ dB, yields slightly better performance when the self-interference coefficient is high, i.e., $\gamma = -100$ dB.

Fig. 8 presents the total energy consumption versus maximal wireless transmission power P. We find that the total energy consumption first decreases dramatically and then decreases smooth with maximal wireless transmission power P. According to Figs. 6 to 8, it is found that HD is always better than FD.
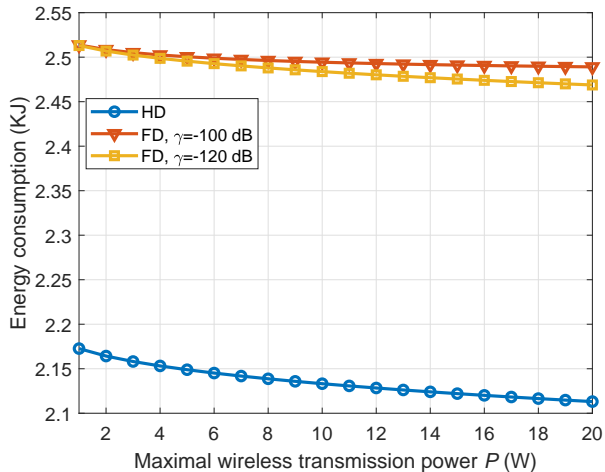
Fig. 8. Energy consumption versus maximal wireless transmission power P.

The reason is that the transmit circuit power consumption of the user is high in FD, while there is only small receive circuit power consumption of the user in the energy harvesting stage of HD mode. As a result, the transmit power of the user in FD is lower than that in HD, which results in longer hovering time and higher energy consumption of the UAV.

VI. CONCLUSION

In this paper, we have investigated the total energy minimization problem for UAV communication with energy harvesting. It is shown that the UAV should stay directly above the user with low height for energy transferring and information reception. It is also found that HD mode is recommended compared to FD mode. The general 3D trajectory optimization for UAV communication with beamforming, instability error, and delay requirements is left for future work.

APPENDIX A
ROTARY-WING UAV PROPULSION ENERGY CONSUMPTION

In this appendix, we derive the propulsion energy consumption model of rotary-wing UAVs. The main notations and typical values used in this appendix are summarized in Table I.

TABLE I
LIST OF MAIN NOTATIONS AND TYPICAL VALUES.

| Notation	Physical meaning	Value
W	UAV weight in Newton	20
ρ	Air density in kg/m^3	1.225
S_{FP}	Fuselage equivalent flat plate area in m^2	0.0151
R	Rotor radius in meter (m)	0.4
A	Rotor disc area in m^2	0.503
Ω	Blade angular velocity in radians/second	300
d_0	Fuselage drag ratio	0.6
s	Rotor solidity	0.05
δ	Profile drag coefficient	0.012
k	Incremental correction factor to induced power	0.1
m	UAV mass in kg	2.04
g	Gravitational acceleration in m/s^2	9.8
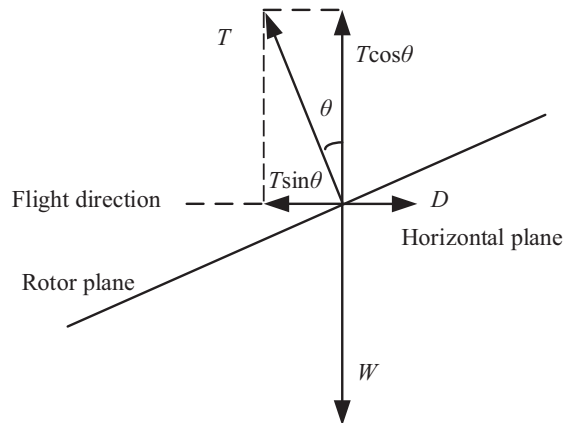
Fig. 9. Schematic of the forces on a UAV with a fixed height and straight flight.

A. Rotary-Wing UAVs in Forward Straight Flight

We first obtain the propulsion energy consumption model with a fixed height and straight flight. Fig. 9 shows the simplified schematics of the longitudinal forces acting on the aircraft with fixed a height [51, Fig. 13.2], which include the following forces: (i) T: rotor thrust, normal to the disc plane and directed upward; (ii) D: fuselage drag, which is in the opposite direction of the aircraft velocity; and (iii) W: aircraft weight. In Fig. 9, θ is the tilt angle of the rotor disc. From Fig. 9, we have the following equation:

$$T\sin\theta - D = ma, \quad W - T\cos\theta = 0, \qquad (\mathrm{A.1})$$

where a denotes the acceleration. According to [52, Eq. (4.5)], the UAV fuselage drag D can be written as

$$D = \frac{1}{2}\rho S_{\mathrm{FP}} V^2. \qquad (\mathrm{A.2})$$

Due to the complexity of deriving the precise power consumption for a rotary-wing aircraft, we assume that the drag coefficient of the blade section is constant [46]. Under some mild assumptions, the propulsion power for rotary-wing UAV with fixed height, speed V and rotor thrust T can be given by [46, Eq. (66)],

$$P_{\mathrm{f}}(V,\kappa) = P_0\left(1 + \frac{3V^2}{\Omega^2 R^2}\right)$$
$$+ P_1\kappa\sqrt{\sqrt{\kappa^2 + \frac{\rho^2 A^2 V^4}{W^2}} - \frac{\rho A V^2}{W}} + \frac{1}{2}d_0\rho s A V^3, \quad (\mathrm{A.3})$$

where

$$\kappa \triangleq \frac{T}{W} \qquad (\mathrm{A.4})$$

is defined as the thrust-to-weight ratio, $P_0 = \frac{\delta}{8}\rho s A\Omega^3 R^3$ and $P_1 = (1+k)\frac{W^{\frac{3}{2}}}{\sqrt{2\rho A}}$.

Based on (A.1), (A.2) and (A.4), we can obtain

$$\kappa = \sqrt{1 + \frac{(\rho S_{\mathrm{FP}} V^2 + 2ma)^2}{4W^2}}. \qquad (\mathrm{A.5})$$

$$E_1(q(t), T_0) = \int_0^{T_0} \left[P_0 \left(1 + c_1 v(t)^2\right) + P_1 \sqrt{1 + (c_2 v(t)^2 + c_3 a(t)v(t))^2} \right.$$
$$\left. \cdot \sqrt{\sqrt{1 + (c_2 v(t)^2 + c_3 a(t)v(t))^2 + c_4^2 v(t)^4} - c_4 v(t)^2} + c_5 v(t)^3 \right] \mathrm{d}t. \qquad (A.8)$$
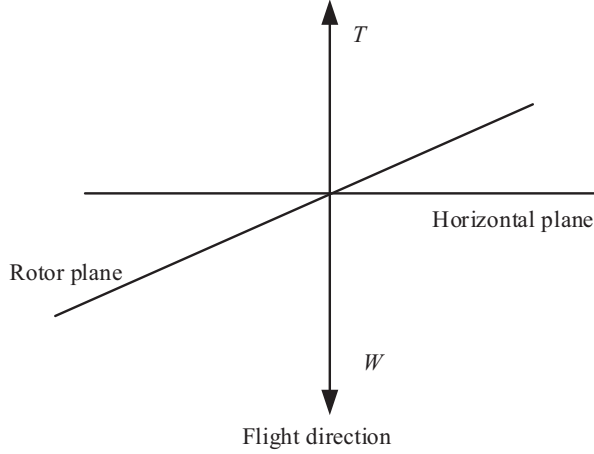

Fig. 10. Schematic of the forces on a UAV in vertical flight.

Substituting (A.5) into (A.3) yields

$$P_f(V, a) = P_0 \left(1 + c_1 V^2\right) + P_1 \sqrt{1 + (c_2 V^2 + c_3 a)^2}$$
$$\times \sqrt{\sqrt{(1 + (c_2 V^2 + c_3 a)^2 + c_4^2 V^4} - c_4 V^2} + c_5 V^3. \qquad (A.6)$$

where

$$c_1 = \frac{3}{\Omega^2 R^2}, c_2 = \frac{\rho S_{\mathrm{FP}}}{2W}, c_3 = \frac{m}{W}, c_4 = \frac{\rho A}{W}, c_5 = \frac{1}{2}d_0\rho s A. \qquad (A.7)$$

For a UAV with trajectory $q(t)$, we have velocity $v(t) = \dot{q}(t)$ and acceleration $a(t) = \ddot{q}(t)$. The total propulsion energy can be expressed as (A.8), as shown in the front of the next page, where T_0 is the time duration.

B. Rotary-Wing UAVs in Vertical Flight

Then, we obtain the propulsion energy consumption model in vertical flight. In Fig. 10, we show the simplified schematics of the longitudinal forces acting on the aircraft with in vertical flight. In vertical flight, it is assumed that the velocity is non-zero only in the vertical direction.

From Fig. 10, we have

$$W - T = ma \qquad (A.9)$$

for vertical descend and

$$T - W = ma \qquad (A.10)$$

for vertical climb.

According to [51, Eqs. (12.13), (12.35)], the total required power for vertical descend is

$$P_c(V, T) = P_2 + \frac{1}{2}TV + \frac{T}{2}\sqrt{V^2 + \frac{2T}{\rho A}}, \qquad (A.11)$$

where $P_2 = \frac{\delta}{8}\rho s A\Omega^3 R^3 + \frac{kW^{\frac{3}{2}}}{\sqrt{2\rho A}}$ and we assume that the acceleration a is smaller than the Gravitational acceleration $g = 9.8$ m/s^2. Substituting $T = W - ma$ to (A.11) yields

$$P_c(V, a) = P_2 + \frac{W - ma}{2}V + \frac{W - ma}{2}\sqrt{V^2 + \frac{2(W - ma)}{\rho A}}. \qquad (A.12)$$

In the vertical descend, the direction of both velocity and acceleration is vertical. The trajectory is one dimensional, which can be expressed by $q(t)$. As a result, the total propulsion energy in vertical descend can be given y

$$E_2(q(t), T_0) = \int_0^{T_0} \left(P_2 + \frac{Wv(t) - ma(t)v(t)}{2} \right.$$
$$\left. + \frac{W - ma(t)}{2}\sqrt{v(t)^2 + \frac{2(W - ma(t))}{\rho A}} \right) \mathrm{d}t$$
$$= P_2 T_0 + \frac{W(q(T_0) - q(0))}{2}$$
$$- \frac{m(v(T_0)^2 - v(0)^2)}{4} + \int_0^{T_0} \frac{W - ma(t)}{2}$$
$$\times \sqrt{v(t)^2 + \frac{2(W - ma(t))}{\rho A}}\mathrm{d}t. \qquad (A.13)$$

According to [51, Eqs. (12.13), (12.51)] and (A.10), the required power for vertical climb can be calculated as

$$P_d(V, a) = P_2 + \frac{W + ma}{2}V + \frac{W + ma}{2}\sqrt{V^2 + \frac{2(W + ma)}{\rho A}}. \qquad (A.14)$$

Thus, the total propulsion energy in vertical climb can be given

by

$$E_4(q(t), T_0) = \int_0^{T_0} \left(P_2 + \frac{Wv(t) + ma(t)v(t)}{2} \right.$$

$$\left. + \frac{W + ma(t)}{2} \sqrt{v(t)^2 + \frac{2(W + ma(t))}{\rho A}} \right) dt$$

$$= P_2 T_0 + \frac{W(q(T_0) - q(0))}{2}$$

$$+ \frac{m(v(T_0)^2 - v(0)^2)}{4} + \int_0^{T_0} \frac{W + ma(t)}{2}$$

$$\times \sqrt{v(t)^2 + \frac{2(W + ma(t))}{\rho A}} dt. \qquad \text{(A.15)}$$

APPENDIX B
PROOF OF THEOREM 1

The dual problem of problem (27) with relaxed constraints can be given by:

$$\max_{\boldsymbol{\beta}, \boldsymbol{\gamma}, \boldsymbol{\lambda}, \boldsymbol{\mu}} \quad D(\boldsymbol{\beta}, \boldsymbol{\gamma}, \boldsymbol{\lambda}, \boldsymbol{\mu}), \qquad \text{(B.1)}$$

where

$$D(\boldsymbol{\beta}, \boldsymbol{\gamma}, \boldsymbol{\lambda}, \boldsymbol{\mu}) = \begin{cases} \min_{\boldsymbol{w}, \boldsymbol{v}} & \mathcal{L}(\boldsymbol{w}, \boldsymbol{v}, \boldsymbol{\beta}, \boldsymbol{\gamma}, \boldsymbol{\lambda}, \boldsymbol{\mu}) \\ \text{s.t.} & \sum_{k=1}^K w_{kl} = 1, \forall l \in \mathcal{K} \\ & w_{kl} \in [0, 1], \forall k, l \in \mathcal{K} \\ & v_{kli} \geq 0, \forall k \in \mathcal{K} \backslash \{1\}, l, i \in \mathcal{K}, \end{cases} \qquad \text{(B.2)}$$

with

$$\mathcal{L}(\boldsymbol{w}, \boldsymbol{v}, \boldsymbol{\beta}, \boldsymbol{\gamma}, \boldsymbol{\lambda}, \boldsymbol{\mu}) = \sum_{l=1}^K w_{1l} E_{0l} + \sum_{k=2}^K \sum_{l=1}^K \sum_{i=1}^K v_{kli}^2 E_{li}$$

$$+ \sum_{l=1}^K w_{Kl} E_{l0} + \sum_{k=1}^K \beta_k \left(\sum_{l=1}^K w_{kl} - 1 \right)$$

$$+ \sum_{k=2}^K \sum_{l=1}^K \sum_{i=1}^K \left[\gamma_{kli}(w_{(k-1)l} + w_{ki} - 1 - v_{kli}) \right.$$

$$\left. + \lambda_{kli}(v_{kli} - w_{(k-1)l}) + \mu_{kli}(v_{kli} - w_{ki}) \right] \quad \text{(B.3)}$$

and $\boldsymbol{\beta} = \{\beta_k\}, \boldsymbol{\gamma} = \{\gamma_{kli}\}, \boldsymbol{\lambda} = \{\lambda_{kli}\}, \boldsymbol{\mu} = \{\mu_{kli}\}$.

To minimize the objective function in (B.2), which is a linear combination of w_{kl}, we should let the smallest association coefficient corresponding to the w_{kl} be 1 among all k with given l. Therefore, the optimal w_{kl}^* is thus given as (28).

To obtain the optimal v_{kli}^* from (B.2), we set the first derivative of objective function to zero, i.e.,

$$\frac{\partial \mathcal{L}(\boldsymbol{w}, \boldsymbol{v}, \boldsymbol{\beta}, \boldsymbol{\gamma}, \boldsymbol{\lambda}, \boldsymbol{\mu})}{\partial v_{kli}} = 2E_{li}v_{kli} - \gamma_{kli} + \lambda_{kli} + \mu_{kli} = 0, \quad \text{(B.4)}$$

which yields $v_{kli} = \frac{\gamma_{kli} - \lambda_{kli} - \mu_{kli}}{2E_{li}}$. Considering constraint $v_{kli} \geq 0$, we can obtain the optimal solution to problem (27) as (29).

APPENDIX C
PROOF OF THEOREM 2

Introducing $t_{k31} = \rho_k t_{k3}$ and $t_{k32} = (1 - \rho_k) t_{k32}$, problem (50) can be equivalent to

$$\min_{t_{k31}, t_{k32}, p_{\pi_k}} \quad t_{k31} + t_{k32} \qquad \text{(C.1a)}$$

$$\text{s.t.} \quad t_{k32} B \log_2 \left(1 + \frac{p_{\pi_k} b h_k^{-\alpha}}{B \sigma^2} \right) \geq D_{\pi_k} \qquad \text{(C.1b)}$$

$$\zeta P b h_k^{-\alpha} t_{k31} \geq t_{k31} p_{\pi_k}^{\text{re}} + t_{k32} \left(p_{\pi_k}^{\text{tr}} + \frac{p_{\pi_k}}{\epsilon_{\pi_k}} \right). \qquad \text{(C.1c)}$$

Observing (C.1), constraint (C.1c) holds with equality for the optimal solution. Based on constraint (C.1c) with equality, we can obtain

$$p_{\pi_k}^* = \frac{\epsilon_{\pi_k}(\zeta P b h_k^{-\alpha} - p_{\pi_k}^{\text{re}}) t_{k31}}{t_{k32}} - \epsilon_{\pi_k} p_{\pi_k}^{\text{tr}}. \qquad \text{(C.2)}$$

Substituting (C.2) into problem (C.1) yields

$$\min_{t_{k31}, t_{k32} \geq 0} \quad t_{k31} + t_{k32} \qquad \text{(C.3a)}$$

$$\text{s.t.} \quad t_{k32} B \log_2 \left(u_1 + \frac{u_2 t_{k31}}{t_{k32}} \right) \geq D_{\pi_k}, \qquad \text{(C.3b)}$$

where u_1 and u_2 are defined in (61). For the optimal solution, constraint (C.3b) always holds with equality, which yields

$$t_{k31}^* = \left(2^{\frac{D_{\pi_k}}{B t_{k32}}} - u_1 \right) \frac{t_{k32}}{u_2}. \qquad \text{(C.4)}$$

Using (C.4), problem (C.3) is simplified to

$$\min_{t_{k32} \geq 0} \quad f(t_{k32}) \triangleq t_2 + \left(2^{\frac{D_{\pi_k}}{B t_{k32}}} - 1 \right) \frac{t_{k32}}{u_2}. \qquad \text{(C.5)}$$

Then,

$$f''(t_{k32}) = \frac{(\ln 2)^2}{u_2 B^2 t_{k32}^3} e^{\frac{(\ln 2) D_{\pi_k}}{B t_{k32}}} \geq 0, \qquad \text{(C.6)}$$

which verifies that problem (C.5) is convex, and the optimal t_{k32} can be obtained by solving $f'(t_{k32}) = 0$. Calculating from (C.5), we have

$$f'(t_{k32}) = 1 - \left(\left(\frac{(\ln 2) D_{\pi_k}}{B t_{k32}} - 1 \right) e^{\frac{(\ln 2) D_{\pi_k}}{B t_{k32}}} + 1 \right) \frac{1}{u_2}, \quad \text{(C.7)}$$

which yields

$$t_{k32}^* = \frac{(\ln 2) D_{\pi_k}}{BW \left(\frac{u_2 - 1}{e} \right) + B}. \qquad \text{(C.8)}$$

As a result, the optimal solution of problem (50) is provided in Theorem 2.

APPENDIX D
PROOF OF THEOREM 3

To minimize problem (52), constraints (52b) and (52c) should hold with equalities for the optimal solution, as otherwise the objective value (52a) can be further decreased, which contradicts that the solution is optimal. Setting (52b) and (52c) with equalities yields

$$p_{\pi_k} = \left(2^{\frac{D}{B(t_{k3} - \delta_{\pi_k})}} - 1 \right) \frac{\gamma P + B \sigma^2}{b h_k^{-\alpha}}. \qquad \text{(D.1)}$$

14

$$p_{\pi_k} = \frac{\epsilon_{\pi_k}(\zeta Pbh_k^{-\alpha} - p_{\pi_k}^{\text{re}})t_{k3}}{t_{k3} - \delta_{\pi_k}} - \epsilon_{\pi_k}p_{\pi_k}^{\text{tr}}. \qquad (D.2)$$

Combining (D.1) and (D.2), the optimal solution of problem (52) is given by (63) and (64).

REFERENCES

[1] Y. Zeng, R. Zhang, and T. J. Lim, "Wireless communications with unmanned aerial vehicles: Opportunities and challenges," *IEEE Commun. Mag.*, vol. 54, no. 5, pp. 36–42, May 2016.

[2] M. Mozaffari, A. T. Z. Kasgari, W. Saad, M. Bennis, and M. Debbah, "Beyond 5G with UAVs: Foundations of a 3D wireless cellular network," *CoRR*, vol. abs/1805.06532, 2018. [Online]. Available: http://arxiv.org/abs/1805.06532

[3] W. Saad, M. Bennis, and M. Chen, "A vision of 6G wireless systems: Applications, trends, technologies, and open research problems," *arXiv preprint arXiv:1902.10265*, 2019.

[4] R. Amorim, H. Nguyen, P. Mogensen, I. Z. Kovács, J. Wigard, and T. B. Sørensen, "Radio channel modeling for UAV communication over cellular networks," *IEEE Wireless Commun. Lett.*, vol. 6, no. 4, pp. 514–517, Aug. 2017.

[5] A. Al-Hourani and K. Gomez, "Modeling cellular-to-UAV path-loss for suburban environments," *IEEE Wireless Commun. Lett.*, vol. 7, no. 1, pp. 82–85, Feb. 2018.

[6] Q. Wu, Y. Zeng, and R. Zhang, "Joint trajectory and communication design for multi-UAV enabled wireless networks," *IEEE Trans. Wireless Commun.*, vol. 17, no. 3, pp. 2109–2121, Mar. 2018.

[7] X. Wang, K. Wang, S. Wu, D. Sheng, H. Jin, K. Yang, and S. Ou, "Dynamic resource scheduling in mobile edge cloud with cloud radio access network," *IEEE Trans. Parallel Distributed Syst.*, pp. 1–1, 2018.

[8] Z. Yang, C. Pan, M. Shikh-Bahaei, W. Xu, M. Chen, M. Elkashlan, and A. Nallanathan, "Joint altitude, beamwidth, location, and bandwidth optimization for UAV-enabled communications," *IEEE Commun. Lett.*, vol. 22, no. 8, pp. 1716–1719, Aug. 2018.

[9] S. Say, H. Inata, J. Liu, and S. Shimamoto, "Priority-based data gathering framework in UAV-assisted wireless sensor networks," *IEEE Sensors J.*, vol. 16, no. 14, pp. 5785–5794, July 2016.

[10] C. Zhan, Y. Zeng, and R. Zhang, "Energy-efficient data collection in UAV enabled wireless sensor network," *IEEE Wireless Commun. Lett.*, vol. 7, no. 3, pp. 328–331, June 2018.

[11] J. Gong, T. Chang, C. Shen, and X. Chen, "Flight time minimization of UAV for data collection over wireless sensor networks," *IEEE J. Sel. Areas Commun.*, pp. 1–1, 2018.

[12] D. Yang, Q. Wu, Y. Zeng, and R. Zhang, "Energy tradeoff in ground-to-UAV communication via trajectory design," *IEEE Trans. Veh. Technol.*, vol. 67, no. 7, pp. 6721–6726, July 2018.

[13] L. Xie, J. Xu, and R. Zhang, "Throughput maximization for UAV-enabled wireless powered communication networks," *IEEE Internet Things J.*, vol. 6, no. 2, pp. 1690–1703, Apr. 2019.

[14] ——, "Throughput maximization for UAV-enabled wireless powered communication networks - invited paper," in *Proc. IEEE Veh. Technol. Conf.*, June 2018, pp. 1–7.

[15] S. Cho, K. Lee, B. Kang, K. Koo, and I. Joe, "Weighted harvest-then-transmit: UAV-enabled wireless powered communication networks," *IEEE Access*, vol. 6, pp. 72 212–72 224, 2018.

[16] F. Wu, D. Yang, L. Xiao, and L. Cuthbert, "Energy consumption and completion time tradeoff in rotary-wing UAV enabled WPCN," *IEEE Access*, pp. 1–1, 2019.

[17] F. Wu, D. Yang, L. Xiao, and L. Cuthbert, "Minimum-throughput maximization for multi-UAV-enabled wireless-powered communication networks," *Sensors*, vol. 19, no. 7, p. 1491, 2019.

[18] J. Xu, Y. Zeng, and R. Zhang, "UAV-enabled wireless power transfer: Trajectory design and energy optimization," *IEEE Trans. Wireless Commun.*, pp. 1–1, 2018.

[19] Y. Hu, X. Yuan, J. Xu, and A. Schmeink, "Optimal 1D trajectory design for UAV-enabled multiuser wireless power transfer," *arXiv preprint arXiv:1811.00471*, 2018.

[20] F. Zhou, Y. Wu, R. Q. Hu, and Y. Qian, "Computation rate maximization in uav-enabled wireless powered mobile-edge computing systems," *IEEE J. Sel. Areas Commun.*, pp. 1–1, 2018.

[21] P. Zhan, K. Yu, and A. L. Swindlehurst, "Wireless relay communications with unmanned aerial vehicles: Performance and optimization," *IEEE Trans. Aerosp. Electron. Syst.*, vol. 47, no. 3, pp. 2068–2085, July 2011.

[22] L. Kong, L. Ye, F. Wu, M. Tao, G. Chen, and A. V. Vasilakos, "Autonomous relay for millimeter-wave wireless communications," *IEEE J. Sel. Areas Commun.*, vol. 35, no. 9, pp. 2127–2136, Sept. 2017.

[23] R. Fan, J. Cui, S. Jin, K. Yang, and J. An, "Optimal node placement and resource allocation for UAV relaying network," *IEEE Commun. Lett.*, vol. 22, no. 4, pp. 808–811, Apr. 2018.

[24] C. Pan, H. Ren, Y. Deng, M. Elkashlan, and A. Nallanathan, "Joint blocklength and location optimization for URLLC-enabled UAV relay systems," *IEEE Commun. Lett.*, vol. 23, no. 3, pp. 498–501, Mar. 2019.

[25] M. Mozaffari, W. Saad, M. Bennis, and M. Debbah, "Unmanned aerial vehicle with underlaid device-to-device communications: Performance and tradeoffs," *IEEE Trans. Wireless Commun.*, vol. 15, no. 6, pp. 3949–3963, June 2016.

[26] N. Zhao, F. Cheng, F. R. Yu, J. Tang, Y. Chen, G. Gui, and H. Sari, "Caching UAV assisted secure transmission in hyper-dense networks based on interference alignment," *IEEE Trans. Commun.*, vol. 66, no. 5, pp. 2281–2294, May 2018.

[27] M. Chen, M. Mozaffari, W. Saad, C. Yin, M. Debbah, and C. S. Hong, "Caching in the sky: Proactive deployment of cache-enabled unmanned aerial vehicles for optimized quality-of-experience," *IEEE J. Sel. Areas Commun.*, vol. 35, no. 5, pp. 1046–1061, May 2017.

[28] Z. Yang, C. Pan, K. Wang, and M. Shikh-Bahaei, "Energy efficient resource allocation in UAV-enabled mobile edge computing networks," *IEEE Trans. Wireless Commun.*, vol. 18, no. 9, pp. 4576–4589, Sep. 2019.

[29] A. Al-Hourani, S. Kandeepan, and S. Lardner, "Optimal LAP altitude for maximum coverage," *IEEE Wireless Commun. Lett.*, vol. 3, no. 6, pp. 569–572, Dec. 2014.

[30] M. Alzenad, A. El-Keyi, F. Lagum, and H. Yanikomeroglu, "3-D placement of an unmanned aerial vehicle base station (UAV-BS) for energy-efficient maximal coverage," *IEEE Wireless Commun. Lett.*, vol. 6, no. 4, pp. 434–437, Aug. 2017.

[31] M. Alzenad, A. El-Keyi, and H. Yanikomeroglu, "3-D placement of an unmanned aerial vehicle base station for maximum coverage of users with different QoS requirements," *IEEE Wireless Commun. Lett.*, vol. 7, no. 1, pp. 38–41, Feb. 2018.

[32] J. Lyu, Y. Zeng, R. Zhang, and T. J. Lim, "Placement optimization of UAV-mounted mobile base stations," *IEEE Commun. Lett.*, vol. 21, no. 3, pp. 604–607, Mar. 2017.

[33] R. I. Bor-Yaliniz, A. El-Keyi, and H. Yanikomeroglu, "Efficient 3-D placement of an aerial base station in next generation cellular networks," in *Proc. IEEE Int. Conf. Commun.*, May 2016, pp. 1–5.

[34] M. Mozaffari, W. Saad, M. Bennis, and M. Debbah, "Efficient deployment of multiple unmanned aerial vehicles for optimal wireless coverage," *IEEE Commun. Lett.*, vol. 20, no. 8, pp. 1647–1650, Aug. 2016.

[35] V. Sharma, R. Sabatini, and S. Ramasamy, "UAVs assisted delay optimization in heterogeneous wireless networks," *IEEE Commun. Lett.*, vol. 20, no. 12, pp. 2526–2529, Dec. 2016.

[36] Q. Wu and R. Zhang, "Common throughput maximization in UAV-enabled OFDMA systems with delay consideration," *IEEE Trans. Commun.*, vol. 66, no. 12, pp. 6614–6627, Dec. 2018.

[37] C. Zhan and Y. Zeng, "Completion time minimization for multi-UAV-enabled data collection," *IEEE Trans. Wireless Commun.*, vol. 18, no. 10, pp. 4859–4872, Oct. 2019.

[38] C. Zhan, Y. Zeng, and R. Zhang, "Trajectory design for distributed estimation in UAV-enabled wireless sensor network," *IEEE Trans. Veh. Technol.*, vol. 67, no. 10, pp. 10 155–10 159, Oct. 2018.

[39] Y. Zeng and R. Zhang, "Energy-efficient UAV communication with trajectory optimization," *IEEE Trans. Wireless Commun.*, vol. 16, no. 6, pp. 3747–3760, June 2017.

[40] H. Ju and R. Zhang, "Optimal resource allocation in full-duplex wireless-powered communication network," *IEEE Trans. Commun.*, vol. 62, no. 10, pp. 3528–3540, Oct. 2014.

[41] Z. Ding, C. Zhong, D. W. K. Ng, M. Peng, H. A. Suraweera, R. Schober, and H. V. Poor, "Application of smart antenna technologies in simultaneous wireless information and power transfer," *IEEE Commun. Mag.*, vol. 53, no. 4, pp. 86–93, Apr. 2015.

[42] X. Zhou, R. Zhang, and C. K. Ho, "Wireless information and power transfer: Architecture design and rate-energy tradeoff," *IEEE Trans. Commun.*, vol. 61, no. 11, pp. 4754–4767, Nov. 2013.

[43] B. Clerckx, R. Zhang, R. Schober, D. W. K. Ng, D. I. Kim, and H. V. Poor, "Fundamentals of wireless information and power transfer: From rf energy harvester models to signal and system designs," *IEEE J. Sel. Areas Commun.*, vol. 37, no. 1, pp. 4–33, Jan. 2019.

[44] J. Kang, I. Kim, and D. I. Kim, "Wireless information and power transfer: Rate-energy tradeoff for nonlinear energy harvesting," *IEEE Trans. Wireless Commun.*, vol. 17, no. 3, pp. 1966–1981, Mar. 2018.

[45] Z. Yang, W. Xu, Y. Pan, C. Pan, and M. Chen, "Optimal fairness-aware time and power allocation in wireless powered communication

networks," *IEEE Trans. Commun.*, vol. 66, no. 7, pp. 3122–3135, July 2018.

[46] Y. Zeng, J. Xu, and R. Zhang, "Energy minimization for wireless communication with rotary-wing uav," *IEEE Trans. Wireless Commun.*, 2019.

[47] S. Boyd and L. Vandenberghe, *Convex Optimization*. Cambridge University Press, 2004.

[48] Z. Yang, W. Xu, J. Shi, H. Xu, and M. Chen, "Association and load optimization with user priorities in load-coupled heterogeneous networks," *IEEE Trans. Wireless Commun.*, vol. 17, no. 1, pp. 324–338, Jan. 2018.

[49] D. P. Bertsekas, *Convex Optimization Theory*. Athena Scientific Belmont, 2009.

[50] Z. Yang, M. Chen, W. Saad, and M. Shikh-Bahaei, "Optimization of rate allocation and power control for rate splitting multiple access (RSMA)," *arXiv preprint arXiv:1903.08068*, 2019.

[51] A. Filippone, *Flight performance of fixed and rotary wing aircraft*. Elsevier, 2006.

[52] A. R. S. Bramwell, D. Balmford, and G. Done, *Bramwell's helicopter dynamics*. Elsevier, 2001.